A Study of Infrared Absorption in the Oxidation of Zinc-Substituted Magnetites to Defect Phase γ and Hematite

B. GILLOT* AND R. M. BENLOUCIF

Laboratoire de Recherches sur la réactivité des Solides associé au CNRS, Faculté des Sciences Mirande, B.P. 138 - 21004 Dijon Cedéx, France

AND A. ROUSSET

Laboratoire de Chimie des Matériaux Inorganiques, Université Paul Sabatier, Toulouse III, 118, route de Narbonne, 31000 Toulouse, France

The effect of substitution extent on formation of superstructure-ordered vacancies in zinc-substituted lacunar spinels of type $(Zn_x^{2+}Fe_{1-x}^{3+})_A(Fe_{(5+x)/3}^{3+}\square_{(1-x)/3})_BO_4^{2-}$ was investigated using ir spectrometry. Only those lacunar phases whose substitution extent x is less than about 0.3 show a vacancy ordering on octahedral sites. In addition, referring to the disappearance of the 635-cm^{-1} absorption band, which is characteristic of these lacunar spinels, we show that the transformation temperature of the γ phases into αFe_2O_3 increases with zinc substitution extent. For the α phase obtained at 700°C we have found a linear variation between the intensity difference of the 390- and 450-cm^{-1} absorption bands and the percentage of αFe_2O_3.

Introduction

Previous studies (*1–3*) using X-ray diffraction and ir spectrometry have shown that the oxidation of finely divided magnetites (crystallite size less than about 3000 Å) substituted by aluminum or chromium of type $(Fe^{2+}Fe_{2-x}^{3+}M_x^{3+})O_4^{2-}$ $(0 < x < 2)$, depending on temperature, resulted either in lacunar phases of similar spinel structure or to corundum structure phases. For lacunar phases $(Fe_{(8-8y)/3}^{3+}M_{8y/3}^{3+}\square_{1/3})O_4^{2-}$ $(0 < y < \frac{2}{3})$ the occurrence of a large number of absorption bands in the region 200–750 cm^{-1} and of a large number of superstructure rays in X-ray diffraction for low-substitution ex-

tents $(y < 0.26)$ confirms a vacancy ordering on the octahedral sites of the spinel lattice. At higher substitution extents ordering disappears and the ir spectrum is characterized by two absorption bands as for inverse spinels.

The transformation of these metastable lacunar phases into rhombohedral phases $\alpha(Fe_{6-y}^{3+}M_y^{3+})O_9^{2-}$ $(0 < y < 6)$ by temperature rise was also followed by ir. For α phases substituted by chromium a linear variation of frequency with the chromium content was observed. This allowed us to identify an unknown compound of type $\alpha(Fe_{6-y}^{3+}Cr_y^{3+})O_9^{2-}$ and it has been established that, in certain temperature conditions and oxidation times, the α phase composition during transformation could differ from that of the corresponding γ phase.

* Author to whom all correspondence should be addressed.

Following this work it seemed of interest to extend the investigation to zinc-substituted magnetites, which also oxidize into lacunar phase for sufficiently small crystallite sizes; these phases may exhibit a vacancy ordering. In addition, the present study is extended to phases obtained by precipitation of αFe_2O_3 from the same lacunar phases during a temperature rise.

Samples and Experimental Methods

The preparation conditions of zinc-substituted magnetites, in principle, do not differ from the previous method used to prepare aluminum or chromium-substituted magnetites (4). The thermal decomposition of mixed iron and zinc oxalates such as $(Fe_{1-x}Zn_x)C_2O_4$, $2H_2O$ ($0 < x < \frac{1}{3}$) leads, through adequate thermal treatments at low temperature ($<500°C$), to the solid solutions $Fe_3O_{4(1-x)}ZnFe_2O_{4(x)}$, which are extremely divided solids and hence largely reactive.

Radiocrystallographic analysis shows that the samples contain only the spinel phase with, sometimes, a small amount of ZnO for high Zn-substitution extents. Only samples with an X-ray pattern free from the ZnO phase were used to carry out the ir studies. The synthesized materials were mixed spinels (Fe^{2+} ions on octahedral sites B and Zn^{2+} ions on tetrahedral sites A)

which show an increase in the lattice parameter with the substitution extent x (Table I). The formula of these compounds may be written:

$$(Zn_x^{2+}Fe_{1-x}^{3+})_A(Fe_{1-x}^{2+}Fe_{1+x}^{3+})_BO_4^{2-}$$
$$(0 < x < 1).$$
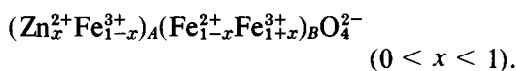
Crystallite size measurements by electron microscopy and from the specific surface show that the samples consist of almost spherical grains of average diameter between 400 and 900 Å, depending on preparation conditions (Table I).

Defect spinels of cubic sesquioxide type are obtained by low-temperature oxidation ($<300°C$) of the previous solid solutions according to the reaction:

$$(Zn_x^{2+}Fe_{1-x}^{2+}Fe_2^{3+})O_4^{2-} + (1 - x)/4O_2 \rightarrow$$
$$x(Zn^{2+}Fe_2^{3+}O_4^{2-}),3/2(1 - x)Fe_2^{3+}O_3^{2-}.$$
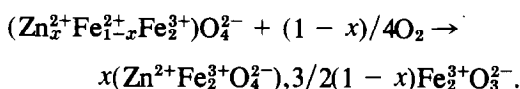
Crystallographic and magnetic studies (5) allow one to attribute the following structural formula to these metastable phases:

$$(Fe_{3(1-x)}^{3+}Zn_{3x}^{2+})_A(Fe_{5+x}^{3+}\square_{1-x})_BO_{12}^{2-}$$
$$(0 < x < 1),$$
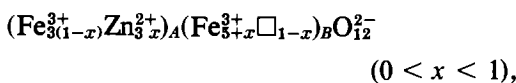
the vacancies being on octahedral sites and zinc on tetrahedral sites. The morphology of these defect spinels is similar to that of the initial phases, in particular the size of the crystallites is the same.

TABLE I

SAMPLE CHARACTERISTICS

Samples $(Zn_x^{2+}Fe_{1-x}^{2+}Fe_2^{3+})O_4^{2-}$	Specific area (m^2/g)	Crystallite mean size (Å)		Lattice parameter (Å)
		Specific area	Electron microscopy	
0	16.3	600	600	8.397
0.15	18	530	500	8.402
0.27	15	650	550	8.409
0.49	11	710	600	8.420
0.76	9.7	830	690	8.427
1	15	600	550	8.440

DTA of the samples was conducted in the presence of air and following thermal rises of 600°C/hr (5). The diagrams obtained show two exothermic phenomena. The former corresponds to the temperature at which the oxidation of the Fe^{2+} ions is maximum; the latter is attributable to the γ cubic-phase transformation obtained after oxidation into the rhombohedral phase α following the reaction:

$$(1 - x)ZnFe_2O_4 - xFe_2O_3 \rightarrow$$

$$(xFe_2O_3) + (1 - x)ZnFe_2O_4.$$
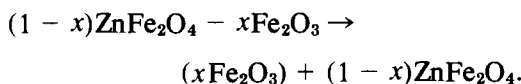
The different oxidations (vs time and vs temperature) were performed in a Setaram MTB 10-8 microbalance.

The ir absorption technique has already been described (1). The spectra were recorded with a Beckman ir 4250 spectrometer over the range 1100–200 cm^{-1}. About 1 mg of sample was mixed and ground with 200 mg CsI before being pelleted under 160 bars pressure.

Results and Discussion

1. Initial Phases $(Zn_x^{2+}Fe_{1-x}^{3+})_A(Fe_{1-x}^{2+}Fe_{1+x}^{3+})_BO_4^{2-}$

In Fig. 1 a number of selected spectra of zinc-substituted magnetites are represented. Conversion of the normal spinel (x = 1) into the inverse spinel (x = 0) is shown on the spectrum by gradual broadening of both high-frequency absorption bands ν_1 and ν_2. In a number of cubic ferrites (1, 6, 7) the absorption ν_1 was detected round 550 cm^{-1} and the absorption ν_2 was detected round 400 cm^{-1}. In zinc-substituted magnetites with varying zinc content, the absorption ν_1 and ν_2 were also detected in the same regions as can be seen from Fig. 1.

The frequency band ν_1 shifted only toward high frequencies as a function of the Fe^{2+} ion content due to the replacement of Fe^{3+} ions by Fe^{2+} ions on the octahedral
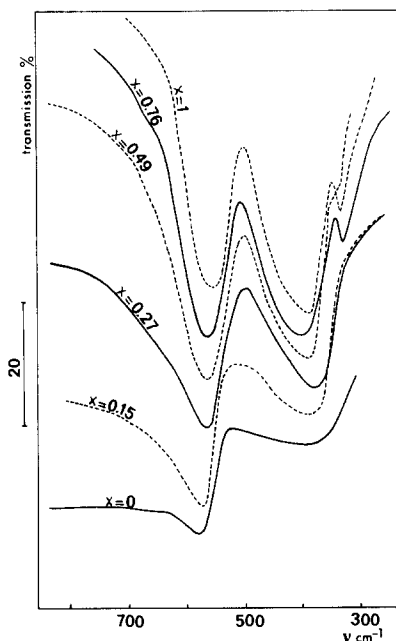

FIG. 1. Infrared spectra of $(Zn_x^{2+}Fe_{1-x}^{3+})_A$ $(Fe_{1-x}^{2+}Fe_{1+x}^{3+})_BO_4^{2-}$ spinels over the range 200–800 cm^{-1}.

sites of the spinel lattice. The two broadened bands observed for low-zinc-substitution extents are typical both of a disordered inverse spinel (two diffuse bands) and of a solid compound containing mobile electrons, responsible for a continuous absorption coinciding with the vibrational absorption. The abnormally high value of electrical conductivity for $x < 0.5$ (8) confirms an electronic exchange made easier by the simultaneous presence of Fe^{2+} and Fe^{3+} ions on octahedral sites.

For high substitution extents ($x > 0.7$) a lower-frequency band (weak and sharp) ν_3 is seen to appear. The ν_4 frequency band could not be observed with our assembly; however, from comparison with other zinc ferrites prepared differently (7, 9) this band should occur around 170 cm^{-1}.

2. Lacunar Phases $(Zn_x^{2+}Fe_{1-x}^{3+})_A$ $(Fe_{(5+x)/3}^{3+}\square_{(1-x)/3})_B O_4^{2-}$
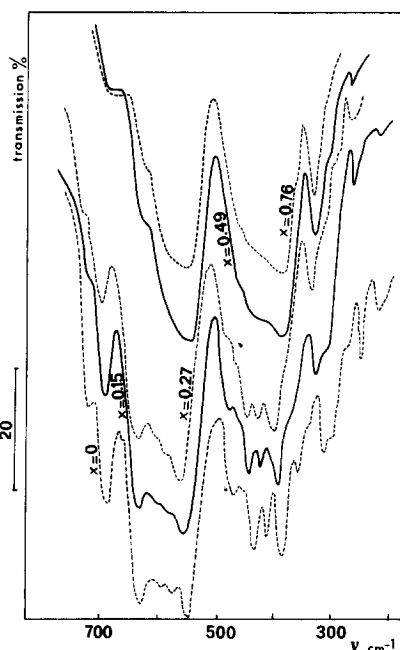
Figure 2 gives the profile of the ir spec-

FIG. 2. Infrared spectra of defect $(Zn_x^{2+}Fe_{1-x}^{3+})_A(Fe_{(5+x)/3}^{3+}\square_{(1-x)/3})O_4^{2-}$ spinels.

trum of the γ phases obtained by oxidizing the previous initial phases at 300°C. For compositions $x < 0.3$ the spectrum differed slightly from pure γFe_2O_3. It showed a relatively high number of absorption bands over the range 200–750 cm^{-1} with 15 infrared absorption peaks occurring at 720, 691, 635, 596, 580, 554, 474, 450, 421, 390, 365, 326, 311, 260, and 220 cm^{-1}. Of these, the peaks at 390, 450, 554 and 635 cm^{-1} were the most intense and are assumed to be due to the stretching vibrations of the Fe–O bonds. The relatively weak intensity of other peaks shall be assumed due to the bending vibrations of the O–Fe–O bonds (2). For $x > 0.3$ the bands of weak intensity disappear progressively and those at 450 and 635 cm^{-1} are only shoulders. The spectrum then is slightly different from that of the initial phase of the same composition x. Referring to the structural formula of these lacunar phases, it is observed that all vacancies are on octahedral sites as for

γFe_2O_3 ($x = 0$), where the number of vacancies is maximum, and, moreover, this number varies with x since it is directly related to the number of Fe^{2+} ions initially present. In the same way, for compositions $x < 0.3$, given the similarity of spectra with γFe_2O_3 (2), the large number of absorption bands may be attributed to the occurrence of a certain order in the vacancy and cation distribution on octahedral sites. Besides, this ordering is confirmed by the presence of superstructure reflections in the X-ray diffraction spectrum. The fact that this ordering remains up to $x = 0.3$, i.e., for a vacancy extent δ higher than 0.23 ($\delta = (1 - x)/3$), is to be related to partially oxidized magnetites where, for an oxidation ratio $\delta > 0.26$, we have also found a large number of absorption bands specific to a vacancy ordering on octahedral sites (2). Indeed, relating the formula of partially oxidized magnetite $(Fe^{3+})_A(Fe_{1+2\delta}^{3+}Fe_{1-3\delta}^{2+}\square_\delta)_BO_4^{2-}$ ($0 < \delta < \frac{1}{3}$) to that of lacunar phases γ, it is noticed that the only difference between both formulae on B sites is the valence of iron cations. Thus it is no wonder that a similarity is found in the ir spectrum for this composition range.

In addition, in both cases, when the vacancy extent decreases, the ordering disappears. This agrees fully with the absence of superstructure reflections in the X-ray diagram along with a considerable change of the ir spectrum, which shows a relatively low number of absorption bands.

3. Precipitation of αFe_2O_3 from γ Lacunar Phases

As for lacunar phases resulting from the oxidation of trivalent ion-substituted magnetites, DTA (5) and electrical conductivity measurement (9, 10) showed an increase in the stability of these γ phases with an increase of the zinc-substituted extent. These phases undergo crystal structure changes on temperature rise. In all cases

there is precipitation of hematite and formation of ferrite according to:

$$(Zn_x^{2+}Fe_{(8-2x)/3}^{3+}\square_{(1-x)/3})O_4^{2-} \rightarrow$$

$$xZn^{2+}Fe_2^{3+}O_4^{2-} + 4/3(1 - x)Fe_2^{3+}O_3^{2-};$$
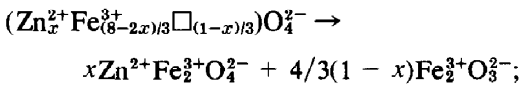
zinc-rich phases are the more stable since temperatures of about 600°C are required in the transformation corresponding to composition $x = 0.76$ against only 400°C for transformation $\gamma(Fe_{8/3}^{3+}\square_{1/3})$ $O_4^{2-} \rightarrow \frac{4}{3}Fe_2^{3+}O_3^{2-}$.

Figure 3 show the ir spectra of both hematite and ferrite phases when the lacunar phases of different composition are heated to 700°C for several hours. The four pure αFe_2O_3 bands at 540, 470, 390, and 320 cm^{-1}, respectively, are always present but during zinc substitution a shift is observed towards the low frequencies of the band at 470 cm^{-1} with its disappearance for pure ferrite. Thus the effect of the ferrite phase seems only to shift this band and cause the intensity of absorption bands of αFe_2O_3 to vary, especially the 390-cm^{-1} band. The intensity difference between the 390- and
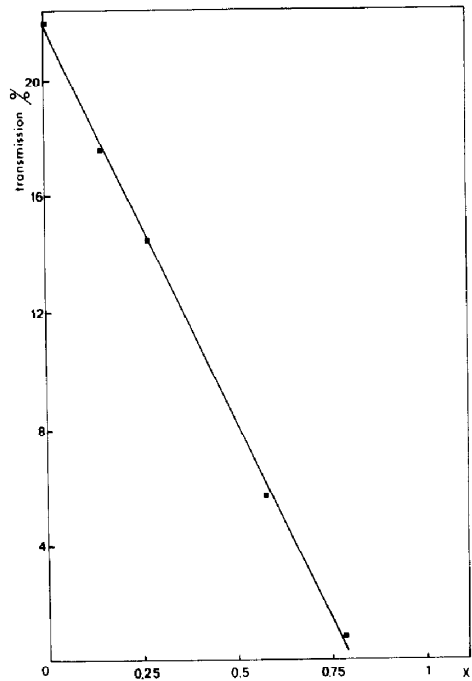

FIG. 4. Evolution of the intensity difference of the 390 and 450 cm^{-1} bands as a function of zinc-substitution extent.
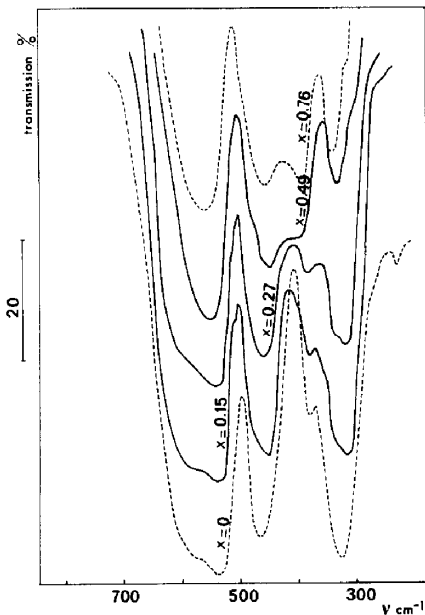

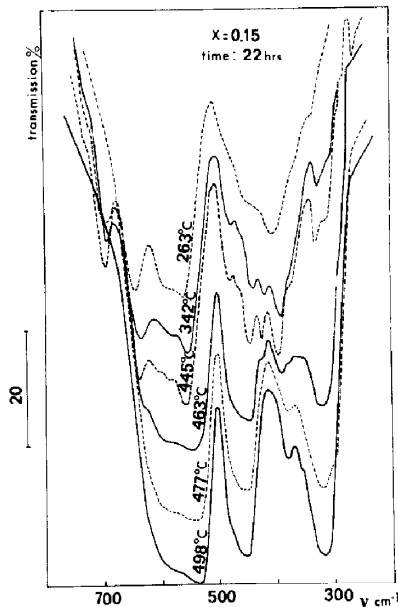FIG. 3. Infrared spectra of αFe_2O_3 + $ZnFe_2O_4$

FIG. 5. Evolution vs temperature of the ir spectrum of the γ phase of composition $x = 0.15$.

the 470-cm^{-1} band results in a linear variation with composition (Fig. 4); hence, it is possible to determine the unknown substitution extent of a zinc-substitution magnetite.

These results show that whatever the substitution extent x the ir spectrum is slightly changed since only the proportion of both phases αFe_2O_3 and $ZnFe_2O_4$ varies but not the composition. The result is that the two strong bands of high frequency at about 550 and 390 cm^{-1}, which must necessarily be assigned to the vibrations of $M^{III}O_6$ octahedral groups (11, 12), are in the absorption range 390–550 cm^{-1} of the group of "condensed" FeO_6 octahedra. This absorption range is also that of the two strong bands of γ lacunar phases (3).

4. Evolution of the Infrared Spectrum vs Temperature and Oxidation Time of the γ Phases

For temperatures less than 700°C but above the oxidation temperature into the γ phase (300°C), the ir spectrum of these γ phases varies with temperature and time. Figures 5, 6, 7 and 8 show the ir spectrum profile during transformation for two largely different compositions: $x = 0.15$ when the γ phases are ordered and $x = 0.76$ when they are not ordered. Whatever the composition, the conversion of the γ phase into the α phase occurs progressively whether as a function of temperature for a given oxidation time (Figs. 5 and 7) or as a function of time for the same temperature (Figs. 6 and 8). It is then possible, by fixing the oxidation time, to evaluate a transition temperature for each composition. For this purpose, it is possible, for example, to refer to the temperature at which the 635 cm^{-1} peak disappears. This peak—although its intensity varies with composition—is characteristic of the γ phase whether it is ordered or not. The variation of the transition temperature with composition (for $x >$ 0.70, the sensitivity of the method depend
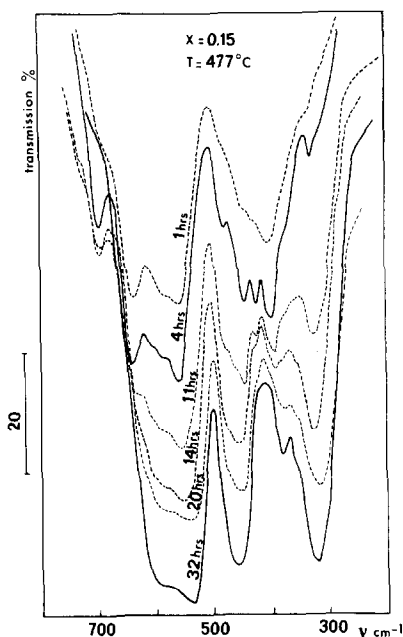

FIG. 6. Evolution vs time of the ir spectrum of the γ phase of composition $x = 0.15$.
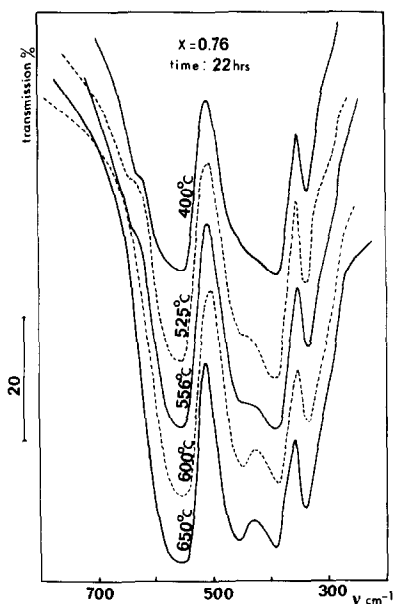

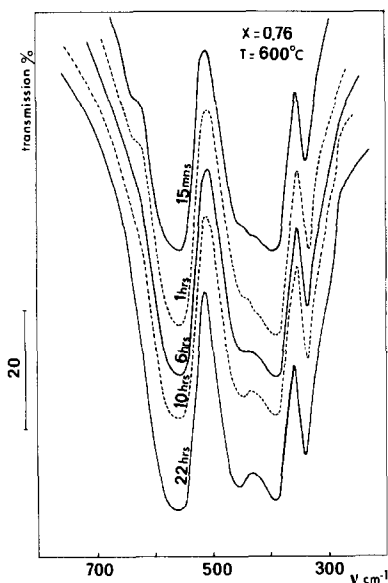FIG. 7. Evolution vs temperature of the ir spectrum of the γ phase of composition $x = 0.76$.

FIG. 8. Evolution vs time of the ir spectrum of the γ phase of composition x = 0.76.

on composition), represented in Fig. 9, expresses an increase in the stability of these γ phases along with the increase of the zinc-substitution extent. A similar change is obtained for conversion temperatures determined by other techniques such as DTA (5, 13) or electrical conductivity (10) (Fig. 9). The differences between transformation temperatures recorded for
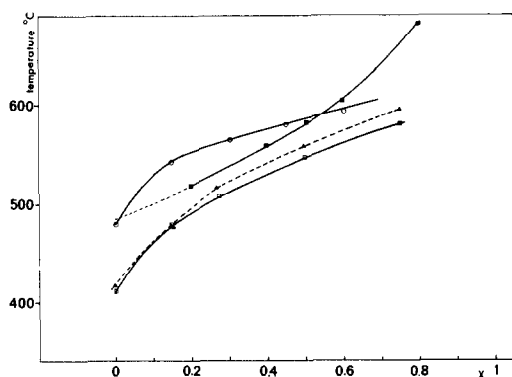

FIG. 9. Effect of composition on precipitation of αFe₂O₃ in Zn ferrous ferrites. □, present study; ▲, by conductivity: Ref. (10); ○, by DTA: Ref. (5); ■, by DTA: Ref. (13).

the different methods results, on the one hand, from the reference selected for transformation (in DTA for example, it is the top of the exothermic peak) and, on the other, from crystallite size (in Ref. (13) crystallite size is around 1 μm).

Conclusion

Infrared and X-ray investigation of the lacunar phases obtained by oxidation of zinc-substituted finely divided magnetites enables us to conclude that, for a given vacancy extent ($\delta > 0.23$), the existence of superstructure rays and a large number of absorption bands agrees with vacancy and cation ordering on octahedral sites. We can, then, state that, following the presence of a relatively low number of absorption bands for substitution extents above $x =$ 0.30, this ordering disappears, which is in full agreement with the total absence of superstructure rays in the X-ray diagram (5). As for the ir spectrum of the α phases resulting from full conversion of γ phases at 700°C, it always shows four absorption bands (apart from pure ferrite) and changes little due to the fact that the transformation always leads to two phases of the same composition, i.e., hematite and ferrite. Since the difference in intensity between the 390- and 450-cm⁻¹ bands varies linearly with the zinc-substitution extent, an unknown composition can be determined. Finally, during the transformation of these γ phases into α phases over the temperature range 400–600°C, we have shown, referring to the disappearance of the 635-cm⁻¹ absorption band, that the stability of these lacunar phases increases with zinc substitution.

References

1. B. GILLOT, F. BOUTON, J. F. FERRIOT, F. CHASSAGNEUX, AND A. ROUSSET, J. Solid State Chem. 21, 375 (1977).

2. B. GILLOT AND F. BOUTON, *J. Solid State Chem.* **32,** 303 (1980).

3. B. GILLOT, F. BOUTON, F. CHASSAGNEUX, AND A. ROUSSET, *J. Solid State Chem.* **33,** 245 (1980).

4. A. ROUSSET, J. PARIS, AND P. MOLLARD, *Ann. Chim.* **7,** 119 (1972).

5. G. DUPRE, A. ROUSSET, AND P. MOLLARD, *Mater. Res. Bull.* **11,** 473 (1976).

6. R. D. WALDRON, *Phys. Rev.* **99,** 1727 (1955).

7. N. W. GRIMES AND A. J. COLLETT, *Nature Phys. Sci.* **230,** 158 (1971).

8. B. GILLOT, R. M. BENLOUCIF, AND A. ROUSSET, *J. Phys. Chem. Solids,* in press.

9. A. MITSUISHI, H. YOSHINAGA, AND S. FUJITA, *J. Phys. Soc. Japan,* **13,** 1236 (1958).

10. B. GILLOT ET R. M. BENLOUCIF, *C.R. Acad. Sci. Paris,* **289,** 341 (1979).

11. J. PREUDHOMME AND P. TARTE, *Spectrochim. Acta A* **27,** 1817 (1971).

12. G. BUSCA, N. COTENA, AND P. F. ROSSI, *Mater. Chem.* **3,** 271 (1978).

13. T. YAMAGUCHI AND T. KIMURA, *J. Amer. Ceram. Soc.* **59,** 333 (1976).